Available online at www.sciencedirect.com

ScienceDirect

International Journal of Mass Spectrometry 272 (2008) 137–148

International Journal of Mass Spectrometry

www.elsevier.com/locate/ijms

A selected ion flow tube study of the reactions of H_3O^+, NO^+ and $O_2^{\bullet+}$ with a series of sesquiterpenes

F. Dhooghe [a,*], C. Amelynck [a], N. Schoon [a], E. Debie [b], P. Bultinck [b], F. Vanhaecke [c]

[a] *Belgian Institute for Space Aeronomy, Ringlaan 3, B-1180 Brussels, Belgium*
[b] *Department of Inorganic and Physical Chemistry, Ghent University, Krijgslaan 281, S3, B-9000 Ghent, Belgium*
[c] *Department of Analytical Chemistry, Ghent University, Krijgslaan 281, S12, B-9000 Ghent, Belgium*

Received 11 December 2007; received in revised form 30 January 2008; accepted 1 February 2008
Available online 13 February 2008

Abstract

Product ion distributions (PIDs) for the reactions of seven sesquiterpenes (aromadendrene, β-caryophyllene, α-cedrene, α-humulene, isolongifolene, longifolene and δ-neoclovene) with H_3O^+, NO^+ and $O_2^{\bullet+}$ reagent ions have been determined in a selected ion flow tube (SIFT) instrument operated at 1.4 mbar and 297 K.

The H_3O^+/sesquiterpene reactions mainly proceed by non-dissociative proton transfer ($C_{15}H_{25}^+$, *m/z* 205), except for the reactions of H_3O^+ with β-caryophyllene and α-humulene which are characterized by more pronounced fragmentation. Two groups of fragment ions of which the components are separated by CH_2 units, are generally observed.

The NO^+/sesquiterpene reactions mainly result in the charge transfer product ($C_{15}H_{24}^+$, *m/z* 204). The NO^+/sesquiterpene charge transfer yield is generally larger than the protonated sesquiterpene yield for the corresponding H_3O^+/sesquiterpene reactions. A small amount of association product ($C_{15}H_{24}\cdot NO^+$, *m/z* 234) is found for the sesquiterpenes aromadendrene, β-caryophyllene, longifolene and δ-neoclovene.

$O_2^{\bullet+}$/sesquiterpene reactions are found to proceed mainly by dissociative charge transfer, resulting in severe fragmentation.

The collisional rate constants for these reactions were calculated using the parameterized theory of Su and Chesnavich, taking into account polarizabilities and electrical dipole moments of the sesquiterpenes as derived from B3LYP/aug-cc-pVDZ quantum chemical calculations.

Experimental rate constants for the reactions of NO^+ and $O_2^{\bullet+}$ with the sesquiterpenes were obtained relatively to the calculated H_3O^+/sesquiterpene rate constants. Absolute H_3O^+/sesquiterpene rate constants were obtained for β-caryophyllene, α-cedrene, α-humulene and longifolene. Large but systematic discrepancies between experimentally determined rate constants and calculated collision rate constants suggest the need for a re-evaluation of sesquiterpene saturation vapor pressure values.

In view of possible detection of sesquiterpenes in moist samples, the influence of water vapor on the ion chemistry was investigated and the reaction rate constants of $H_3O^+\cdot H_2O$ and $NO^+\cdot H_2O$ with sesquiterpenes were obtained relative to those of bare H_3O^+ and NO^+, respectively.

Keywords: SIFT; Ion/molecule reactions; Sesquiterpenes; Proton transfer; Charge transfer

1. Introduction

Large amounts of non-methane volatile organic compounds (NMVOCs) are emitted from terrestrial vegetation every year (about 1150 Tg/year worldwide) [1] and it is widely accepted that they have a significant impact on atmospheric chemistry. Terpenes are an important class of these biogenic volatile organic compounds (BVOCs). They are biosynthetically derived from units of isoprene (C_5H_8, 2-methyl-1,3-butadiene) and have the chemical structure $(C_5H_8)_n$, where n is the number of isoprene units. The BVOCs studied here (sesquiterpenes) belong to a group of terpenes that consist of three isoprene units and thus have the molecular formula $C_{15}H_{24}$. Sesquiterpenes can be acyclic, endocyclic or exocyclic and their emissions from vegetation vary greatly according to time of year, type of vegetation, etc. Although minor attention has been devoted to sesquiterpene emissions from vegetation in comparison to isoprene and monoterpenes, recent studies have shown that for some types of vegetation sesquiterpene emissions can be considerable [2,3].

---

[*] Corresponding author. Tel.: +32 27 90 39 17; fax: +32 2 374 84 23.
E-mail address: frederik.dhooghe@aeronomie.be (F. Dhooghe).

1387-3806/$ – see front matter © 2008 Elsevier B.V. All rights reserved.
doi:10.1016/j.ijms.2008.02.002

Sesquiterpenes have a very short atmospheric lifetime (minutes to days) because of their high reactivity with atmospheric oxidants like O_3, OH and NO_3 [4], resulting in very low ambient concentrations. Atmospheric oxidation of sesquiterpenes mainly leads to the formation of low-volatile substances, which may condense on pre-existing particles and contribute to secondary organic aerosols (SOA) [5,6]. The contribution of sesquiterpene oxidation products to SOA is presently considered as a hot research topic.

Mass spectrometry techniques have often been used for sesquiterpene detection. Most frequently, Gas Chromatography–Mass Spectrometry (GC–MS) [7–10] has been used. In this technique, compounds are chromatographically separated before being detected by mass spectrometry. In GC/MS, analyte molecules are ionized by electron impact (EI) at a typical collision energy of 70 eV. This is a highly energetic ionization method, which results in extensive fragmentation of the molecules being studied. Detection and quantification of gas molecules that are present in low concentrations requires long pre-concentration steps, during which analyte molecules are collected on an adsorbant medium. In a second phase the adsorbed species are released by thermodesorption, separated by GC, ionized and mass analyzed. Because of this pre-concentration step, GC–MS does not have a good time resolution and this may be inconvenient when monitoring rapidly varying emissions of reactive trace compounds, such as sesquiterpenes.

A possible solution to this problem is the application of Chemical Ionization Mass Spectrometry (CIMS) techniques, in which ionization of the analyte molecules is achieved through fast exothermic ion/molecule reactions. As less excess energy is available for fragmentation, chemical ionization (CI) is generally considered as a soft ionization method. Because of its high sensitivity, the CIMS technique can be used for the instantaneous on-line detection and quantification of trace compounds, i.e., without any time-consuming pre-concentration step. Proton Transfer Reaction Mass Spectrometry [11] (PTR-MS), a well-established, highly sensitive and fast analytical drift-tube CIMS technique, which uses H_3O^+ reagent ions and allows the detection of many volatile organic compounds (VOCs), has recently also been applied to measure sesquiterpene concentrations [12]. Reaction of H_3O^+ ions with many VOCs mainly results in the protonated VOC, but the H_3O^+/sesquiterpene interaction in a PTR-MS reactor at typical drift-tube conditions is known to proceed through both dissociative and non-dissociative proton transfer, resulting in multiple fragment ion species. This fragmentation results in a decrease of the detection efficiency with respect to other VOCs which are not or hardly subjected to fragmentation following protonation.

The aim of this study is to find out whether other reagent ion species than H_3O^+ may lead to higher detection efficiencies of sesquiterpenes. Moreover, other CIMS techniques such as Selected Ion Flow Tube Mass Spectrometry [13] (SIFT-MS), are sometimes successful in distinguishing isomers by alternately using different source ions (H_3O^+, NO^+ and $O_2^{\bullet+}$), which may result in important differences in the ion chemistry of different isomers and therefore lead to their selective detection. For this reason, the ion chemistry of H_3O^+, NO^+ and $O_2^{\bullet+}$ with seven sesquiterpenes has been studied in a well-validated selected ion flow tube instrument. The product ion distribution (PID) and the influence of water vapor on the product ion spectrum were determined for each of the sesquiterpenes investigated. The chemical structures of the sesquiterpenes studied can be found in Fig. 1. We are well aware that the product ion distributions of the studied ion/molecule reactions obtained at thermal conditions in the SIFT flow tube reactor cannot be simply used in PTR-MS applications, but they give at least an indication of the degree of fragmentation and the fragment ion masses that can be expected in a drift-tube reactor. The study of the reactions of NO^+ and $O_2^{\bullet+}$ with sesquiterpenes is also interesting in view of a possible future role of these reagent ion species in drift-tube CIMS instrumentation [14].

2. Experimental

2.1. Instrumental

In this study, a SIFT has been used to investigate the ion chemistry of H_3O^+, NO^+ and $O_2^{\bullet+}$ ions with a series of sesquiterpenes

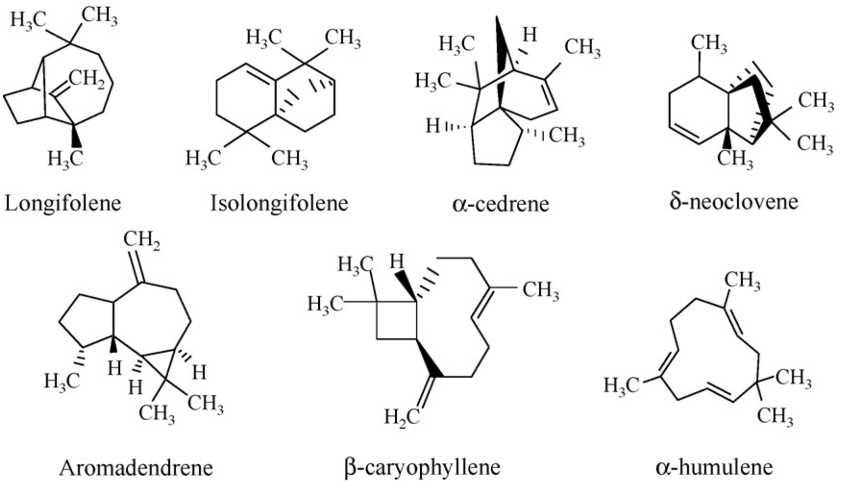

Fig. 1. Chemical structures of sesquiterpenes investigated in this study.

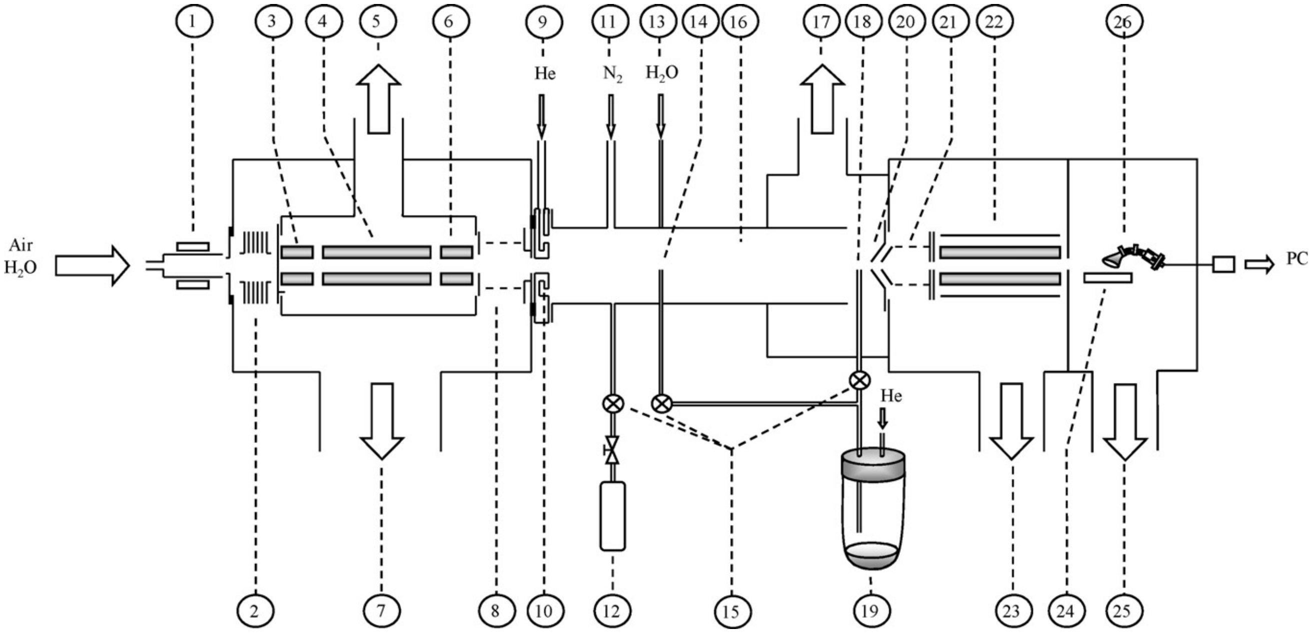

Fig. 2. SIFT instrument schematics: (1) microwave discharge, (2) ion inlet lens, (3) selection quadrupole pre-filter, (4) selection quadrupole, (5) to 500 L s^{-1} turbomolecular pump, (6) selection quadrupole post-filter, (7) to 1600 L s^{-1} turbomolecular pump, (8) exit ion lens, (9) inlet main carrier gas, (10) SIFT venturi inlet, (11) N_2 inlet, (12) inlet for mass discrimination, (13) water inlet, (14) kinetics inlet, (15) needle valves, (16) flow tube, (17) to Roots blower, (18) inlet for PIDs, (19) sesquiterpene reservoir, (20) biased ion inlet flange, (21) ion inlet lens, (22) analyzer quadrupole, (23) to three 300 L s^{-1} turbomolecular pumps, (24) conversion dynode, (25) to turbomolecular pump 300 L s^{-1}, and (26) Channeltron detector.

at room temperature (297 K) and a pressure of 1.4 mbar. The instrument used in these experiments is an upgraded version of the SIFT which has been described in earlier publications [15–17]. A schematic representation of the instrument is given in Fig. 2.

The source ions are created in a microwave discharge in a mixture of air and water vapor by means of an Evenson type cavity. They are subsequently extracted from the discharge region and guided towards the differentially pumped selection quadrupole mass filter by means of a set of electrostatic lens elements. The mass-selected ions leaving the selection quadrupole are guided towards the SIFT injector and injected into a helium carrier gas flow (100 STP $cm^3 s^{-1}$), which is maintained by a large Roots blower backed by a rotary vane pump. The ions are convectively transported in the flow tube reactor by this helium gas flow. A small nitrogen flow is added a few cm downstream the SIFT injector to quench vibrationally excited reagent ions. The stainless steel flow tube has a diameter of 4.0 cm, a total length of 50.7 cm and is provided with four reactant gas inlets. A first inlet, at 40.0 cm from the sampling orifice, is used for mass discrimination measurements. The second and third inlet are positioned opposite each other at 27.0 cm from the sampling orifice and are, respectively, used for kinetic measurements and for adding water vapor to evaluate the influence of water on the ion chemistry in the flow tube. A last inlet, located at 0.8 cm from the sampling orifice, is used to obtain product ion distributions. At the downstream end of the flow tube, the source and product ions are sampled through an orifice in a conically shaped biased inlet flange and they are subsequently guided towards the detection quadrupole mass filter by means of an electrostatic lens system. Ions that are transmitted by the mass filter are accelerated towards a conversion dynode at high negative potential (−5 kV). Electrons leaving the dynode surface after ion impact are then accelerated towards the trumpet of the Channeltron electron multiplier, which is operated in the pulse counting mode. With respect to the previous configuration, the mass spectrometer vacuum chamber has been changed in such a way that the ion detection region is now pumped separately from the analyzer region. This results in a much better vacuum in the detection region. With the new type of ion detector, mass discrimination is less dependent on the high voltage across the Channeltron and because of the better vacuum, the lifetime of the detector is expected to increase considerably.

2.2. Measuring methods

Because of the low vapor pressures and the sticky nature of sesquiterpenes, absolute rate constant measurements of ion/sesquiterpene reactions are rather difficult to perform. We nevertheless measured the reaction rate constants of H_3O^+ ions with four sesquiterpenes by taking into account a value for their vapor pressure ($P_{\mathrm{vap,sesq}}$) at 25 °C as derived from chromatographic retention indices [18]. A low amount of liquid sesquiterpene was stored in a glass reservoir and kept completely immersed in a thermostatically controlled water bath at 25 °C. A small helium flow ($Q_{\mathrm{He,res}}$), sent through water-immersed copper tubing at 25 °C, was blown over the liquid sesquiterpene surface. The resulting diluted sesquiterpene flow was sent through a needle valve and some (¼) in. stainless steel tubing of minimal length, all heated to 90 °C, before being introduced into the flow tube reactor. By changing the conductance of the needle valve, the helium pressure above the sesquiterpene (P_{res}), and therefore also the sesquiterpene mixing ratio in the reactant gas flow, could be varied in a reproducible way. The sesquiterpene flow Q_{sesq}, which enters the flow tube reactor, is given by the formula:

$$Q_{\text{sesq}} = Q_{\text{He, res}} \frac{P_{\text{vap, sesq}}}{P_{\text{res}}} \quad (Q_{\text{sesq}} << Q_{\text{He, res}}) \tag{1}$$

For fixed settings of the helium flow rate, the helium pressures above the reservoir and upstream of the copper gas line were measured simultaneously at different needle valve positions by using capacitance manometers. In order to reduce the surface area which was in contact with the sesquiterpene vapor, the manometer above the reservoir was removed when the reservoir contained liquid sesquiterpene. In this case, the pressure above the reservoir P_{res} was deduced from the relationship between the pressure above the reservoir and the pressure upstream of the copper gas line at a fixed helium flow setting and with an empty reservoir.

Rate constants of H_3O^+ ions with sesquiterpenes were obtained from the logarithmic decay of the reagent ion signal as a function of the sesquiterpene concentration in the flow tube, according to the formula:

$$\ln\left(\frac{[H_3O^+]}{[H_3O^+]_0}\right) = -k\tau[C_{15}H_{24}] \tag{2}$$

In this formula square brackets denote concentrations and $[H_3O^+]_0$ refers to the H_3O^+ concentration in the absence of the reactant gas. The reaction time τ is measured experimentally and has a value of 2.65 ms at typical conditions of flow and pressure in the SIFT reactor. $[C_{15}H_{24}]$ is derived from the ratio of Q_{sesq} to the helium buffer gas flow and the total pressure in the SIFT flow tube.

Rate constants for the reactions of NO^+ and $O_2^{\bullet+}$ with sesquiterpenes are obtained relative to the rate constant for H_3O^+. To accomplish this, H_3O^+, NO^+ and $O_2^{\bullet+}$ ions are injected simultaneously into the SIFT reactor by putting the ion selection quadrupole in the total ion mode (RF-only mode). The analyzing quadrupole switches between the 3 ions at different settings of the sesquiterpene flow.

Product ion distributions were obtained by introducing the sesquiterpene at the inlet close to the sampling orifice. This reduces diffusion enhancement effects and possible secondary reactions. The PIDs are acquired by operating the instrument in the multi-ion mode (MIM). Mass discrimination effects are taken into account by using a mass discrimination curve, obtained according to the method described by Španěl and Smith [19]. By introducing sufficient amounts of some very specific volatile organic compounds in the SIFT reactor, the ion composition at the mass spectrometer inlet solely consists of one terminal ion species, for instance MH^+ in the case of the aromatic species benzene, toluene and *m*-xylene and M_2H^+ for the ketones acetone, 2-butanone and 3-pentanone. The mass discrimination factor (MDF) for these ions is then obtained by measuring the ratio of the count rate for the terminal ion species to the terminal ion current on the mass spectrometer inlet plate relative to this ratio obtained for H_3O^+ ions. A mass discrimination curve (MDF as a function of *m*/*z*) is fitted through these points.

In this study, 3-hexanone and 4-heptanone have been included in this series. These gases are also found to form one terminal ion species (M_2H^+) and are therefore suitable to extend the MDF range towards higher *m*/*z* values. Branching ratios have been corrected for isotopic abundance.

In order to study the effect of the presence of water vapor on the ion chemistry, the rate constants of the reactions of $H_3O^+\cdot H_2O$ and $NO^+\cdot H_2O$ ions with the sesquiterpenes were measured relative to those of H_3O^+ and NO^+ respectively, using the method described by Michel et al. [20]. The monohydrated precursor ions $H_3O^+\cdot H_2O$ and $NO^+\cdot H_2O$ ions were created by adding water vapor at the inlet just opposite the kinetic measurements reactant inlet. Hydration of the fragment ions was evaluated by comparing the mass spectra obtained for the sesquiterpenes when no water vapor was present to the spectra obtained when fixed amounts of water vapor were introduced.

2.3. Chemicals

Aromadendrene (97%), isolongifolene (98%), α-humulene (98%), δ-neoclovene (98%), β-caryophyllene (98.5%), longifolene (99%) and α-cedrene (99%) were all purchased from Fluka. Helium used as main carrier gas was obtained from Air Products and is of BIP grade (99.9997%).

3. Results and discussion

3.1. Reaction rate constants

3.1.1. Collision rate constant calculations

The collision rate constants k_C of the ion/sesquiterpene reactions have been calculated with the parameterized equation of Su and Chesnavich [21,22] and are listed in Table 1. In this parameterized theory k_C is given by:

$$k_C = k_L C(\alpha, \mu_D, T) \tag{3}$$

and k_L is given by the Langevin formula:

$$k_L = 2\pi|q|\sqrt{\frac{\alpha}{\mu}} \tag{4}$$

where q is the charge of the ion, α the polarizability, μ_D the electrical dipole moment of the reactant molecule and μ the reduced mass of the ion/molecule system. Since no literature data are available for μ_D and α, these parameters were obtained from quantum chemical calculations. The calculations were performed in a distributed computer environment using Gaussian03 [23]. To take into account all possible molecular conformations, a detailed conformational analysis was carried out by combining a MMFF [24,25] random search with a MM3/MM4 [26,27] stochastic search [28,29]. The minima that were found were optimized at the B3LYP/6-31G(d,p) level and the Hessian was calculated to ensure that all located stationary points were minima. All the minima within an energy window of 4 kcal mole^{-1} were then re-optimized with the aug-cc-pVDZ basis set, and μ_D and α were calculated for each minimum. Collision rate constants were calculated for all individual conformations of a

Table 1
Polarizability, dipole moment and reaction rate constants of the sesquiterpenes

Molecule	μ_D (D)[a]	α (Å^3)[a]	$k_{exp,rel}$ [k_C] ($k_{exp,abs}$) (10^{-9} molecule^{-1} cm^3 s^{-1})				
			H_3O^+	$H_3O^+{\cdot}H_2O$[b]	NO^+[b]	$NO^+{\cdot}H_2O$[b]	$O_2^{\bullet+}$[b]
Aromadendrene	0.60	26.0 {26.0}	[3.0]	2.6 [2.3]	2.6 [2.4]	2.5 [2.0]	2.5 [2.4]
β-Caryophyllene	0.65	26.6 {26.5}	[3.1] (6.1)	2.5 [2.3]	2.7 [2.5]	2.5 [2.0]	2.6 [2.4]
α-Cedrene	0.21	25.3 {26.0}	[2.9] (6.5)	2.4 [2.1]	2.5 [2.3]	2.3 [1.9]	2.4 [2.3]
α-Humulene	0.24	27.4 {27.0}	[3.0] (7.2)	2.5 [2.2]	2.6 [2.4]	2.4 [2.0]	2.5 [2.4]
Isolongifolene	0.22	25.2 {26.0}	[2.9]	2.4 [2.1]	2.4 [2.3]	2.3 [1.9]	2.4 [2.3]
Longifolene	0.94	25.9 {26.0}	[3.2] (6.4)	2.5 [2.4]	2.8 [2.5]	2.6 [2.1]	2.7 [2.5]
δ-Neoclovene	0.28	25.1 {26.0}	[2.9]	2.4 [2.1]	2.5 [2.3]	2.3 [2.1]	2.4 [2.3]

( ): Measured absolute reaction rate constants. { }: Calculated polarizabilities with the method of Miller and Savchik [32]. [ ]: Calculated collisional reaction rates (Su and Chesnavich [21,22]).

[a] Values obtained from B3LYP/aug-cc-pVDZ calculations.

[b] Reaction rate constants have been experimentally derived by obtaining the relative decay rates as described in Section 2.2.

compound using Eq. (3) and subsequently Boltzmann-averaged using the enthalpy to obtain conformational populations. The enthalpy was calculated at 295.15 K and 1.5 mbar via DFT using the standard expressions [30]. Vibrational frequencies were scaled by a factor 0.970 [31].

The polarizability α has also been calculated using an empirical method developed by Miller and Savchik [32]. It has the functional form

$$\alpha(\mathrm{ahc}) = \frac{4}{N}\left[\sum_{A}\tau_A\right]^2, \qquad (5)$$

where N is the number of electrons in the molecule and τ_A is the atomic hybrid component for an atom in a particular hybrid configuration. The summation of these components over all atoms A in the molecule results in the polarizability.

The values of μ_D, α, k_C for the sesquiterpenes listed in Table 1 are all Boltzmann-averaged values over all relevant conformations. Values of α obtained with the method of Miller and Savchik can also be found in this table. The agreement between the polarizability values obtained with both methods is excellent.

3.1.2. Experimentally determined rate constants

Absolute rate constant measurements were carried out for the reactions of H_3O^+ ions with β-caryophyllene, α-humulene, α-cedrene and longifolene.

The values for the rate constants, which are derived from our measurements, are also shown in Table 1 and they vary between 6.1×10^{-9} and 7.2×10^{-9} cm^3 molecule^{-1} s^{-1}, which is about a factor of two too high with respect to the calculated collision rate constant values.

Several reasons can be put forward to try to explain possible errors in rate constant determinations with the present experimental set-up for introducing low vapor pressure compounds.

One reason could be that the evaporation of the sesquiterpene is not fast enough, so that the sesquiterpene pressure above the liquid sample is smaller than the sesquiterpene saturation vapor pressure at the temperature of the reservoir. Therefore, different settings of $Q_{He,res}$, the He flow that is sent over the reservoir, were used (0.17, 0.33 and 0.50 STP cm^3 s^{-1}) and for each setting of $Q_{He,res}$ different sesquiterpene concentrations in the flow tube reactor were realized by varying P_{res} between 6 and 80 mbar (by changing the position of the needle valve). Exponential decay curves over two decades were obtained for the H_3O^+ signal versus sesquiterpene concentration in the flow tube. The rate constants for the ion/sesquiterpene reactions which were derived by using formula (2) are reproducible and independent of $Q_{He,res}$. This indicates that the sesquiterpene vapor pressure above the liquid reservoir is independent of the He flow, which is blown over the reservoir. Moreover, if the evaporation of the liquid sesquiterpene would not be fast enough, the experimentally determined rate constants are expected to be lower than the collision rate constants instead of higher.

Another source of error could be the presence of impurities in the liquid sesquiterpenes with a higher vapor pressure than that of the sesquiterpenes. However, when using H_3O^+ precursor ions and introducing for instance α-cedrene, the resulting product ion spectrum almost solely consists of the protonated sesquiterpene (94%), and therefore, the possible presence of impurities cannot explain at all the high rate constant values that were measured.

Erroneous rate constant determinations can also be explained by condensation problems in the inlet lines. These were avoided by heating the lines and the needle valve between the reservoir and the flow tube.

An important parameter, which to a great extent determines the absolute value of the experimentally obtained rate constants, is the saturation vapor pressure of the sesquiterpenes. We used the data reported by Helmig et al. [18] which, to the best of our knowledge, are the only data available in the literature. In the article of Helmig et al., the saturated vapor pressures were estimated by correlating the linear programmed gas chromatography retention index to the calculated vapor pressures of an *n*-alkane series. Possible errors may be introduced due to the differences between sesquiterpenes and *n*-alkanes.

Exothermic proton transfer reactions are known to proceed at the collision rate. However, because of the lack of thermochemical data for sesquiterpenes, the exothermicity of the ion/sesquiterpene reactions cannot be calculated.

Measurements of the NO^+ and $O_2^{\bullet+}$/sesquiterpene reaction rates relative to the H_3O^+ reaction rate are found to scale with the inverse square root of the reduced mass of the collision partner, indicating that all reactions, which are reported here, proceed at the collision limit.

Previous measurements performed in our lab for exothermic proton transfer reaction rate constants, for which the determination of the absolute reactant concentration was straightforward, generally were found to agree very well with the calculated collision rates. Therefore, the reaction rate constants of NO^+ and $O_2^{\bullet+}$ for the sesquiterpenes investigated are reported relative to the calculated H_3O^+/sesquiterpene reaction rate in Table 1. This table also shows the reaction rate constants for $H_3O^+\cdot H_2O$ and $NO^+\cdot H_2O$, measured relatively with respect to H_3O^+ and NO^+, respectively.

The precision and accuracy for the absolute rate constant values are 9 and 25% respectively, but they do not take into account the error on the vapor pressure values, for which no values have been reported. The precision of the relative rate constants is better than 10%.

3.2. Product ion distributions

In Table 2 an overview of the product ions of the reactions of H_3O^+, NO^+ and $O_2^{\bullet+}$ with the sesquiterpenes studied is given. Only ions with a yield of 2% or more are included in this table.

Table 2
Product ion distributions for the sesquiterpenes studied, corrected for mass discrimination and isotopic abundance

Compound	H_3O^+			NO^+			$O_2^{\bullet+}$		
	m/z	Ion	%	*m/z*	Ion	%	*m/z*	Ion	%
Aromadendrene	95	$C_7H_{11}^+$	3	204	$C_{15}H_{24}^{\bullet+}$	94	94	$C_7H_{10}^{\bullet+}$	2
	109	$C_8H_{13}^+$	3		Others	6	108	$C_8H_{12}^{\bullet+}$	2
	123	$C_9H_{15}^+$	2				121	$C_9H_{13}^+$	4
	135	$C_{10}H_{15}^+$	2				122	$C_9H_{14}^{\bullet+}$	3
	149	$C_{11}H_{17}^+$	8				133	$C_{10}H_{13}^+$	3
	205	$C_{15}H_{25}^+$	80				135	$C_{10}H_{15}^+$	4
		Others	2				147	$C_{11}H_{15}^+$	4
							148	$C_{11}H_{16}^{\bullet+}$	5
							149	$C_{11}H_{17}^+$	2
							161	$C_{12}H_{17}^+$	21
							189	$C_{14}H_{21}^+$	10
							204	$C_{15}H_{24}^{\bullet+}$	21
								Others	19
β-Caryophyllene	81	$C_6H_9^+$	4	80	$C_6H_8^{\bullet+}$	2	93	$C_7H_9^+$	3
	95	$C_7H_{11}^+$	9	134	$C_{10}H_{14}^{\bullet+}$	2	94	$C_7H_{10}^{\bullet+}$	2
	109	$C_8H_{13}^+$	10	148	$C_{11}H_{16}^{\bullet+}$	6	106	$C_8H_{10}^{\bullet+}$	2
	121	$C_9H_{13}^+$	3	161	$C_{12}H_{17}^+$	7	107	$C_8H_{11}^+$	2
	123	$C_9H_{15}^+$	7	176	$C_{13}H_{20}^{\bullet+}$	3	109	$C_8H_{13}^+$	3
	135	$C_{10}H_{15}^+$	8	189	$C_{14}H_{21}^+$	5	119	$C_9H_{11}^+$	2
	137	$C_{10}H_{17}^+$	7	204	$C_{15}H_{24}^{\bullet+}$	59	120	$C_9H_{12}^{\bullet+}$	6
	149	$C_{11}H_{17}^+$	16		Others	16	121	$C_9H_{13}^+$	2
	205	$C_{15}H_{25}^+$	30				122	$C_9H_{14}^{\bullet+}$	2
		Others	6				133	$C_{10}H_{13}^+$	9
							134	$C_{10}H_{14}^{\bullet+}$	3
							135	$C_{10}H_{15}^+$	3
							136	$C_{10}H_{16}^{\bullet+}$	2
							146	$C_{11}H_{14}^{\bullet+}$	5
							147	$C_{11}H_{15}^+$	10
							160	$C_{12}H_{16}^{\bullet+}$	9
							163	$C_{12}H_{19}^+$	2
							175	$C_{13}H_{19}^+$	2
							189	$C_{14}H_{21}^+$	7
							204	$C_{15}H_{24}^{\bullet+}$	9
								Others	15
α-Cedrene	109	$C_8H_{13}^+$	2	204	$C_{15}H_{24}^{\bullet+}$	98	108	$C_8H_{12}^{\bullet+}$	2
	205	$C_{15}H_{25}^+$	94		Others	2	119	$C_9H_{11}^+$	26
		Others	4				120	$C_9H_{12}^{\bullet+}$	2
							136	$C_{10}H_{16}^{\bullet+}$	4
							147	$C_{11}H_{15}^+$	5
							148	$C_{11}H_{16}^{\bullet+}$	2
							161	$C_{12}H_{15}^+$	12
							189	$C_{14}H_{21}^+$	3
							204	$C_{15}H_{24}^{\bullet+}$	35
								Others	9

Table 2 (*Continued*)

Compound	H_3O^+			NO^+			$O_2^{\bullet+}$		
	m/z	Ion	%	*m/z*	Ion	%	*m/z*	Ion	%
α-Humulene	81	$C_6H_9^+$	2	147	$C_{11}H_{15}^+$	11	80	$C_6H_8^{\bullet+}$	7
	95	$C_7H_{11}^+$	7	204	$C_{15}H_{24}^{\bullet+}$	77	82	$C_6H_{10}^{\bullet+}$	3
	109	$C_8H_{13}^+$	7		Others	12	92	$C_7H_8^{\bullet+}$	6
	121	$C_9H_{13}^+$	2				93	$C_7H_9^+$	11
	123	$C_9H_{15}^+$	7				94	$C_7H_{10}^{\bullet+}$	2
	135	$C_{10}H_{15}^+$	4				95	$C_7H_{11}^+$	2
	137	$C_{10}H_{17}^+$	2				107	$C_8H_{11}^+$	2
	149	$C_{11}H_{17}^+$	9				108	$C_8H_{12}^{\bullet+}$	2
	205	$C_{15}H_{25}^+$	54				109	$C_8H_{13}^+$	5
		Others	6				119	$C_9H_{11}^+$	3
							121	$C_9H_{13}^+$	4
							122	$C_9H_{14}^{\bullet+}$	7
							134	$C_{10}H_{14}^{\bullet+}$	2
							135	$C_{10}H_{15}^+$	3
							147	$C_{11}H_{15}^+$	4
							148	$C_{11}H_{16}^{\bullet+}$	4
							161	$C_{12}H_{17}^+$	3
							189	$C_{14}H_{21}^+$	3
							204	$C_{15}H_{24}^{\bullet+}$	6
								Others	8
Isolongifolene	149	$C_{11}H_{17}^+$	2	204	$C_{15}H_{24}^{\bullet+}$	99	148	$C_{11}H_{16}^{\bullet+}$	13
	205	$C_{15}H_{25}^+$	97		Others	1	161	$C_{12}H_{17}^+$	36
		Others	1				175	$C_{13}H_{19}^+$	14
							189	$C_{14}H_{21}^+$	8
							204	$C_{15}H_{24}^{\bullet+}$	28
								Others	1
Longifolene	95	$C_7H_{11}^+$	3	204	$C_{15}H_{24}^{\bullet+}$	93	94	$C_7H_{10}^{\bullet+}$	6
	109	$C_8H_{13}^+$	3	234	$(NO\cdot C_{15}H_{24})^+$	3	95	$C_7H_{11}^+$	2
	149	$C_{11}H_{17}^+$	5		Others	4	108	$C_8H_{12}^{\bullet+}$	3
	205	$C_{15}H_{25}^+$	83				109	$C_8H_{13}^+$	3
		Others	6				120	$C_9H_{12}^+$	2
							122	$C_9H_{14}^{\bullet+}$	2
							134	$C_{10}H_{14}^{\bullet+}$	2
							135	$C_{10}H_{15}^+$	3
							147	$C_{11}H_{15}^+$	2
							148	$C_{11}H_{16}^{\bullet+}$	2
							161	$C_{12}H_{17}^+$	14
							175	$C_{13}H_{19}^+$	3
							176	$C_{13}H_{20}^{\bullet+}$	2
							189	$C_{14}H_{21}^+$	12
							204	$C_{15}H_{24}^{\bullet+}$	26
								Others	16
δ-Neoclovene	95	$C_7H_{11}^+$	3	161	$C_{12}H_{17}^+$	3	106	$C_8H_{10}^{\bullet+}$	5
	109	$C_8H_{13}^+$	3	204	$C_{15}H_{24}^{\bullet+}$	94	119	$C_9H_{11}^+$	3
	123	$C_9H_{15}^+$	2		Others	3	120	$C_9H_{12}^{\bullet+}$	13
	135	$C_{10}H_{15}^+$	2				121	$C_9H_{13}^+$	4
	149	$C_{11}H_{17}^+$	8				122	$C_9H_{14}^{\bullet+}$	4
	205	$C_{15}H_{25}^+$	79				134	$C_{10}H_{14}^{\bullet+}$	12
		Others	3				148	$C_{11}H_{16}^{\bullet+}$	3
							161	$C_{12}H_{17}^+$	4
							162	$C_{12}H_{18}^{\bullet+}$	16
							189	$C_{14}H_{21}^+$	5
							204	$C_{15}H_{24}^{\bullet+}$	19
								Others	12

3.2.1. H_3O^+ reactions

The reactions of all seven sesquiterpenes with H_3O^+ proceed via exothermic proton transfer. This results in the formation of nascent $(C_{15}H_{25}{}^+)^*$ product ions:

$$H_3O^+ + C_{15}H_{24} \rightarrow (C_{15}H_{25}{}^+)^* + H_2O \tag{6}$$

The excited $C_{15}H_{25}{}^{+*}$ ions either stabilize through collisions with the helium buffer gas,

$$(C_{15}H_{25}{}^+)^* + He \rightarrow C_{15}H_{25}{}^+ + He, \tag{7}$$

or decompose into fragment ions.

The reactions of H_3O^+ with isolongifolene and α-cedrene almost exclusively proceed by non-dissociative proton transfer (>94%). Some more fragmentation is observed for the reactions of H_3O^+ with aromadendrene, longifolene and δ-neoclovene, but the protonated sesquiterpene yield is still 79% or more. Non-dissociative proton transfer, however, is less efficient for the reaction of H_3O^+ with β-caryophyllene and α-humulene, which respectively have a protonated sesquiterpene yield of 30 and 54%.

For isolongifolene and α-cedrene only one non-negligible fragment ion was observed. This fragment ion is situated at *m/z* 149 ($C_{11}H_{17}{}^+$) for isolongifolene and at *m/z* 109 ($C_8H_{13}{}^+$) for α-cedrene.

All other H_3O^+/sesquiterpene reactions studied result in multiple fragments that can be divided in 2 groups of which all components are separated by a CH_2 unit (14 u). A first group contains ions with *m/z* 149, 135 and 121 and a second one contains ions with *m/z* 137, 123, 109, 95 and 81.

When introducing a real air sample with a certain humidity hydration of the fragment ions can occur which results in formation of H_2O cluster ions:

$$M^+ + H_2O + He \rightarrow (M^+{\cdot}H_2O) + He \tag{8}$$

However, no occurrence of H_2O cluster ions was found for the sesquiterpenes studied, indicating that the product ion distribution is independent of the relative humidity for these H_3O^+/sesquiterpene reactions. This confirms previous observations that hydrocarbon fragments do not associate with water vapor to form hydrates [33,34].

A comparison between the fragment ions obtained with SIFT-MS in this study and the fragment ions obtained with PTR-MS by Lee et al. [12] for the sesquiterpenes aromadendrene, β-caryophyllene, α-humulene and longifolene can be found in Table 3. A rough indication of the ion intensities relative to the intensity of the molecular ion at *m/z* 205 ($C_{15}H_{25}{}^+$) can also be found in this table. The fragment ions reported by Lee et al. have not been corrected for isotopic abundance.

For aromadendrene, α-humulene and longifolene, more fragment ions are encountered with PTR-MS than with SIFT-MS. Some of these are due to the lack of isotopic correction. Others are a result of the more severe fragmentation taking place in a drift field type instrument like PTR-MS. For β-caryophyllene, two fragment ions at *m/z* 123 ($C_9H_{15}{}^+$) and *m/z* 135 ($C_{10}H_{15}{}^+$) are found with SIFT-MS that have not been encountered by PTR-MS.

3.2.2. NO^+ reactions

NO^+ mainly reacts with the sesquiterpenes studied by charge transfer. Charge transfer with ground state NO^+ is possible for molecules having an ionization energy (IE) smaller than the NO

Table 3
Comparison between fragment ions and intensities obtained in this research (SIFT-MS) and those reported by Lee et al. [12] (PTR-MS)

Aromadendrene		β-Caryophyllene		α-Humulene		Longifolene	
SIFT-MS	PTR-MS	SIFT-MS	PTR-MS	SIFT-MS	PTR-MS	SIFT-MS	PTR-MS
			67		67		
			68				
		81	**81**	81	**81**		81
			82		82		82
95	95	**95**	95	95	95	95	**95**
	96				96		96
					97		
	103				103		103
109	109	**109**	**109**	109	**109**	109	**109**
	110				110		110
	121	121	**121**	121	121		121
123	123	**123**		123	**123**	123	123
	124						124
135	135	**135**		135	135	135	135
	136						136
		137	**137**	137	137		
149	**149**	**149**	**149**	149	**149**	149	**149**
	150				150		150
	163						
205	**205**	**205**	205	**205**	**205**	**205**	**205**
	206		206		206		206
	207						207

Bold: Ions >20% of the unfragmented protonated sesquiterpene ion intensity.

IE of 9.26 eV:

$$NO^{+} + C_{15}H_{24} \rightarrow C_{15}H_{24}{}^{\bullet +} NO \qquad (9)$$

The charge transfer product for aromadendrene, α-cedrene, isolongifolene, longifolene and δ-neoclovene has a yield of 93% or more and thus little fragmentation is observed. For β-caryophyllene and α-humulene, a yield of 59 and

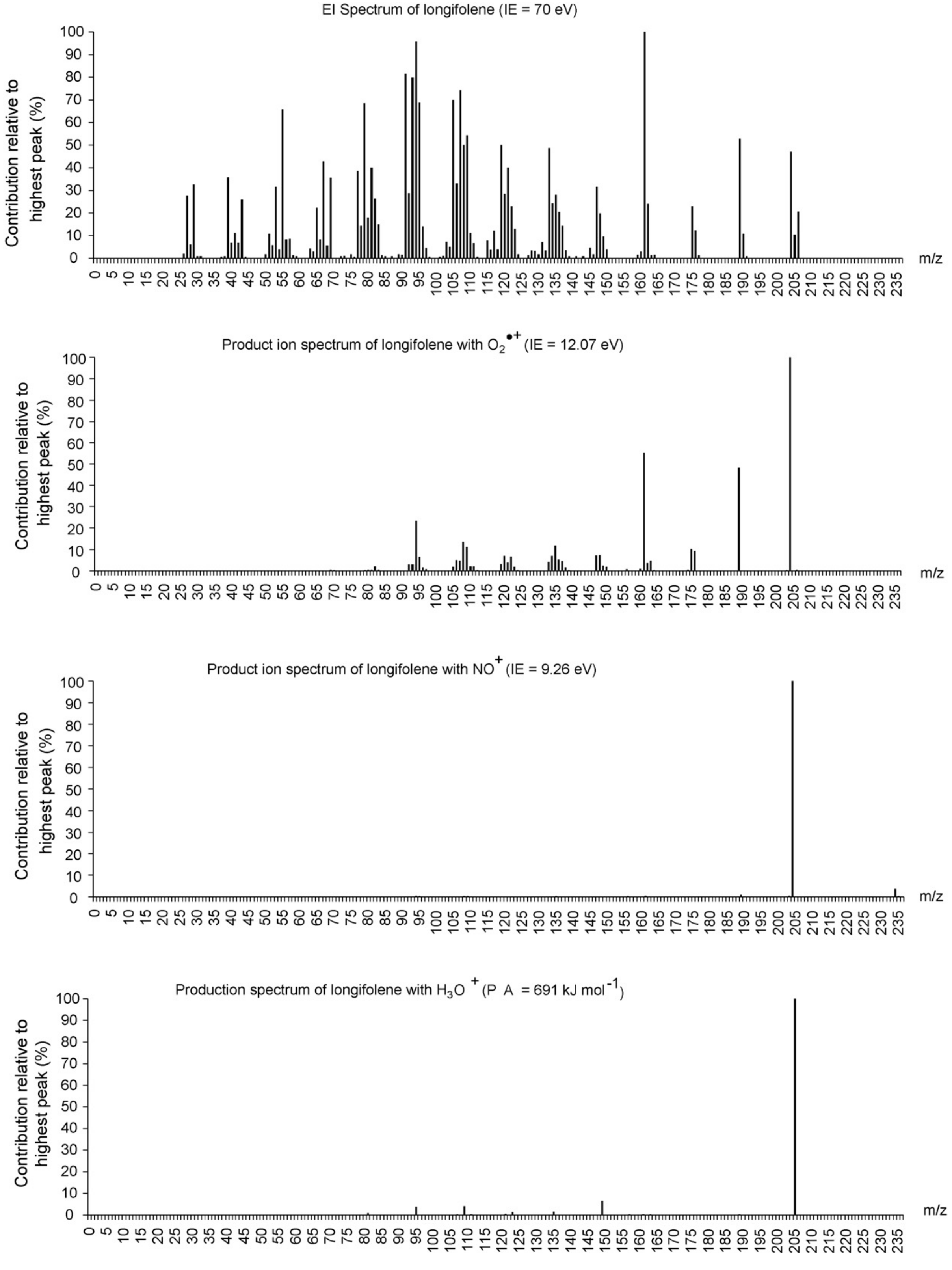

Fig. 3. Product ion spectra for longifolene: EI [38], $O_2{}^{\bullet +}$, NO^+ and H_3O^+.

77%, respectively, has been observed for the molecular ion.

The presence of the charge transfer channel indicates that for all sesquiterpenes studied here, the IE is expected to be below 9.26 eV. However, the IE reported for α-humulene by Martin et al. through photoelectron spectroscopy is 9.54 eV [35]. The presence of the molecular ion cannot be due to reaction with excited NO^{+*} precursor ions, as precautions have been made to eliminate excited states of NO^+ by adding a small amount of N_2 to the main carrier gas. However, when taking into account the uncertainty on the IE, the thermal spread of the ion/molecule interaction energies under SIFT conditions and the possible entropy change for bimolecular reactions, charge transfer with ground state NO^+ cannot be excluded.

NO^+ is also found to react by three-body association, resulting in the formation of the association product at *m*/*z* 234:

$$NO^+ + C_{15}H_{24} \rightarrow (NO{\cdot}C_{15}H_{24})^{+*} \qquad (10)$$

$$(NO{\cdot}C_{15}H_{24})^{+*} + He \rightarrow (NO{\cdot}C_{15}H_{24})^+ + He \qquad (11)$$

Aromadendrene (1%), β-caryophyllene (1%), longifolene (3%) and δ-neoclovene (1%) all show a small amount of the association product.

Apart from the charge transfer product ion and the association product ions, some fragment ions are also observed. These fragment ions can be categorized in 3 groups of which all elements are separated by a CH_2 unit (14 u). A first group contains ions with *m*/*z* 148, 134 and 120. The *m*/*z* values for the ions of the second group are 136, 122, 108, 94 and 80 and the last group contains ions with *m*/*z* 189, 175 and 161.

Except for β-caryophyllene and α-humulene, all these fragments ions have very small yields (<1%).

For β-caryophyllene, a fragment at mass 148 ($C_{11}H_{16}^+$) can be found with a non-negligible yield (6%) and for α-humulene, a fragment ion at *m*/*z* 147 ($C_{11}H_{15}^+$) with a considerable yield (11%) can be found. Because the yield of these two fragment ions is considerable, they may possibly be used to distinguish β-caryophyllene from α-humulene.

Also, β-caryophyllene is the only sesquiterpene of the seven studied that has a small fragment ion at *m*/*z* 220 (1%). This fragment ion most probably results from elimination of a CH_2 unit from the nascent excited $(NO{\cdot}C_{15}H_{24})^{+*}$ adduct:

$$(NO{\cdot}C_{15}H_{24})^{+*} \rightarrow (NO{\cdot}C_{14}H_{22})^+ + CH_2 \qquad (12)$$

Fragment ion hydration was evaluated for the NO^+/sesquiterpene reactions. No fragment ion H_2O clusters were observed for the sesquiterpenes studied. However, the yield of the association product at *m*/*z* 234 is seen to increase as a function of the water vapor concentration. Introducing water vapor results in the formation of the hydrated reagent ion $NO^+{\cdot}H_2O$. Dependent on exothermicity, processes like ligand switching (13) and charge transfer (14) can occur [36]:

$$NO^+{\cdot}H_2O + C_{15}H_{24} \rightarrow (NO{\cdot}C_{15}H_{24})^+ + H_2O \qquad (13)$$

$$NO^+{\cdot}H_2O + C_{15}H_{24} \rightarrow C_{15}H_{24}^+ + NO + H_2O \qquad (14)$$

As the IE reported for α-humulene is slightly higher than the one of NO and the NO^+–H_2O binding energy equals 0.72 eV [37], reaction (14) is not expected to occur for this compound.

3.2.3. $O_2^{\bullet +}$ reactions

Since the IE of O_2 (12.07 eV) is higher than the IE of NO (9.26 eV), more energy is available for fragmentation. As a result, the non-dissociative charge transfer product of the reaction of $O_2^{\bullet +}$ with sesquiterpenes has a yield of less than 35%.

$$O_2^{\bullet +} + C_{15}H_{24} \rightarrow C_{15}H_{24}^{\bullet +} + O_2 \qquad (15)$$

The relative intensities of the fragment ions clearly vary from sesquiterpene to sesquiterpene, but due to the absence of compound-specific fragment ions, identification of individual sesquiterpenes in a mixture of sesquiterpenes cannot be accomplished with O_2^+. The sensitivity for sesquiterpene quantification is hampered by the fact that the molecular ion at *m*/*z* 204 is not always the product ion with the greatest intensity, as can be seen for aromadendrene, β-caryophyllene, α-humulene and isolongifolene (Fig. 2).

Very few electron impact ionization spectra are available for sesquiterpenes. Of the ones studied here, only the spectra for α-humulene and longifolene could be found [38]. In Fig. 3, the spectrum of longifolene resulting from electron impact ionization (EI) is compared to the spectra obtained for chemical ionization with $O_2^{\bullet +}$, NO^+ and H_3O^+. By comparing the occurrence and intensities of the fragment ions for EI and CI, less fragmentation can be observed for the CI spectra. This is to be expected as less energy is available for fragmentation. All fragments observed in the $O_2^{\bullet +}$ spectrum can be found in the EI spectrum.

Of the chemical ionization techniques used, $O_2^{\bullet +}$ results in the most severe fragmentation and H_3O^+ and NO^+ are found to result in only minor fragmentation for longifolene.

4. Conclusions

The absolute rate measurements of H_3O^+ with the sesquiterpenes β-caryophyllene, α-cedrene, α-humulene and longifolene were found to be a factor of two higher than the calculated collision rate constant values. After careful evaluation of possible error causes, it was concluded that the saturated vapor pressure has the largest impact on the values of the experimentally determined rate constants. A good agreement between the calculated collision rate constants and the experimentally determined reaction rate constants would imply that the sesquiterpene saturation vapor pressures at 25 °C reported by Helmig et al. [18] would on average be too low by a factor of two. Given the importance of these data for quantifying sesquiterpene fluxes emitted by vegetation, we believe there is an urgent need for additional sesquiterpene saturation vapor pressure measurements.

The product ion distributions for the reactions of three reagent ions (H_3O^+, NO^+ and $O_2^{\bullet +}$) with seven sesquiterpenes were obtained in this research.

4.1. Feasibility for sesquiterpene quantification

For the H_3O^+/sesquiterpene reactions the protonated sesquiterpene yield ($C_{15}H_{25}^+$, *m/z* 205) is found to differ greatly for the investigated sesquiterpenes. Especially β-caryophyllene and α-humulene are found to undergo severe fragmentation. From the comparison between our SIFT-MS results to the previously reported PTR-MS results for four sesquiterpenes by Lee et al. [12], we expect the fragmentation of sesquiterpenes in a PTR-MS to be at least equivalent to the fragmentation encountered with SIFT-MS and to be dependent on the drift field conditions. Therefore, care should be taken when using the signal at *m/z* 205 for sesquiterpene quantification.

The charge transfer product ($C_{15}H_{24}^+$, *m/z* 204) yields of the NO^+/sesquiterpene reactions are generally found to be larger than the protonated molecule yield ($C_{15}H_{25}^+$, *m/z* 205) observed for the H_3O^+/sesquiterpene reactions. Thus, the $C_{15}H_{24}^+$ signal will provide a better estimate for the sesquiterpene emissions, as it will be influenced to a lesser extent by the differences in yield for the individual sesquiterpenes. NO^+ clearly appears to be the best precursor ion to measure sesquiterpenes with SIFT-MS.

Detection of sesquiterpenes by H_3O^+ and NO^+ does not seem to be hampered by the presence of water vapor.

The $O_2^{\bullet+}$/sesquiterpene reactions result in severe fragmentation and provide large differences in the yields of charge transfer products for all sesquiterpenes studied. This reagent ion can therefore not be used for sesquiterpene quantification.

4.2. Suitability for sesquiterpene differentiation

No characteristic fragment ions were encountered for the H_3O^+/sesquiterpene reactions, so H_3O^+ ions cannot be used to distinguish sesquiterpene isomers.

For the NO^+/sesquiterpene reactions of β-caryophyllene and α-humulene a $C_{11}H_{16}^+$ fragment (*m/z* 148) and a $C_{11}H_{15}^+$ fragment (*m/z* 147) was found, respectively. These fragment ions have considerable yields and can be used as a means of β-caryophyllene and α-humulene distinction, provided that no other NO^+/BVOC reactions result in one of these two specific fragment ions. However, as only seven sesquiterpenes have been investigated in this study, more research is needed to evaluate the feasibility of NO^+ for sesquiterpene isomer distinction. Also, the association product ($C_{15}H_{24}NO^+$, *m/z* 234) has been observed at small yields for aromadendrene, β-caryophyllene, longifolene and δ-neoclovene.

Because of the severe fragmentation encountered for the $O_2^{\bullet+}$/sesquiterpene reactions, the $O_2^{\bullet+}$ reaction spectrum of a realistic air sample is expected to be very complex and suffering from major interference problems. Therefore, no qualitative information can be obtained with $O_2^{\bullet+}$.

4.3. Interference on monoterpene measurements

For the H_3O^+/sesquiterpene reactions fragment ions $C_{10}H_{17}^+$ (*m/z* 137) and $C_6H_9^+$ (*m/z* 81) were found for β-caryophyllene and α-humulene. These ions were previously reported when measuring monoterpenes ($C_{10}H_{16}$) with H_3O^+ [15,39,40]. Sesquiterpene emissions may therefore interfere with monoterpene quantification measurements when using H_3O^+ as reagent ion.

On the other hand, no $C_{10}H_{16}^+$ fragment ions for the NO^+/sesquiterpene reactions were found for the seven sesquiterpenes investigated. This ion has previously been reported to be the major product ion for NO^+/monoterpene reactions. This implies that no interference will occur when measuring air samples containing both monoterpenes and sesquiterpenes when using NO^+ as reagent ion.

Acknowledgements

The authors gratefully acknowledge the support of the Belgian Federal Science Policy Office (Project # MO/35/022). E. Debie is a Research Assistant of the Fund for Scientific Research-Flanders (Belgium) (F.W.O-Vlaanderen).

References

[1] A. Guenther, C.N. Hewitt, D. Erickson, R. Fall, C. Geron, T. Graedel, P. Harley, L. Klinger, M. Lerdau, W.A. McKay, T. Pierce, B. Scholes, R. Steinbrecher, R. Tallamraju, J. Taylor, P. Zimmerman, J. Geophys. Res. 100 (D5) (1995) 8873.

[2] N.C. Bouvier-Brown, R. Holzinger, K. Pallitzsch, A.H. Goldstein, Geophys. Res. Abstr. 9 (2007) 02422 Sref-ID: 1607–7962/gra/EGU2007-A-02422.

[3] T.M. Ruuskanen, H. Hakola, M.K. Kajos, H. Hellén, V. Tarvainen, J. Rinne, Atmos. Environ. 41 (2007) 5807.

[4] R. Atkinson, J. Arey, Atmos. Environ. (Suppl. 2) (2003) S197.

[5] R.J. Griffin, D.R. Cocker III, R.C. Flagan, J.H. Seinfeld, J. Geophys. Res. 104 (D3) (1999) 3555.

[6] N.L. Ng, J.H. Kroll, M.D. Keywood, R. Bahreini, V. Varutbangkul, R.C. Flagan, J.H. Seinfeld, Environ. Sci. Technol. 40 (2006) 2283.

[7] D. Helmig, F. Bocquet, J. Pollmann, T. Revermann, Atmos. Environ. 38 (2004) 557.

[8] C. Holzke, T. Hoffmann, L. Jaeger, R. Koppmann, W. Zimmer, Atmos. Environ. 40 (2006) 3174.

[9] H. Hakola, V. Tarvainen, J. Bäck, H. Ranta, B. Bonn, J. Rinne, M. Kulmala, Biogeosciences 3 (2006) 93.

[10] N.C. Bouvier-Brown, R. Holzinger, K. Palitzsch, A.H. Goldstein, J. Chromatogr. A 1161 (2007) 113.

[11] W. Lindinger, A. Hansel, A. Jordan, Int. J. Mass Spectrom. Ion Process. 73 (1998) 191.

[12] A. Lee, A.H. Goldstein, J.H. Kroll, N.L. Ng, V. Varutbangkul, R.C. Flagan, J.H. Seinfeld, J. Geophys. Res. 111 (D17305) (2006), doi:10.1029/2006JD007050.

[13] D. Smith, N.G. Adams, Adv. Atom. Mol. Phys. 24 (1988) 1.

[14] K.P. Wyche, R.S. Blake, K.A. Willis, P.S. Monks, A.M. Ellis, Rapid Comm. Mass Spectrom. 19 (2005) 3356.

[15] N. Schoon, C. Amelynck, L. Vereecken, E. Arijs, Int. J. Mass Spectrom. 229 (2003) 231.

[16] C. Amelynck, N. Schoon, T. Kuppens, P. Bultinck, E. Arijs, Int. J. Mass Spectrom. 147 (2005) 1.

[17] N. Schoon, C. Amelynck, E. Debie, P. Bultinck, E. Arijs, Int. J. Mass Spectrom. 263 (2007) 127.

[18] D. Helmig, T. Revermann, J. Pollmann, O. Kaltschmidt, A.J. Hernàndez, F. Bocquet, D. David, J. Chromatogr. A 1002 (2003) 193.

[19] P. Španěl, D. Smith, J. Am. Soc. Mass Spectrom. 12 (2001) 863.

[20] E. Michel, N. Schoon, C. Amelynck, C. Guimbaud, V. Catoire, E. Arijs, Int. J. Mass Spectrom. 244 (2005) 50.

[21] T. Su, W.J. Chesnavich, J. Chem. Phys. 76 (1982) 5183.

[22] T. Su, J. Chem. Phys. 89 (1988) 5355.

[23] M.J. Frish, G.W. Trucks, H.B. Schlegel, G.E. Scuseria, M.A. Robb, J.R. Cheeseman, J.A. Montgomery Jr., T. Vreven, K.N. Kudin, J.C. Burant, J.M. Millam, S.S. Iyengar, J. Tomasi, V. Barone, B. Mennucci, M. Cossi, G. Scalmani, N. Rega, G.A. Petersson, H. Natkatsuji, M. Hada, M. Ehara, K. Toyota, R. Fukuda, J. Hasegawa, M. Ishida, T. Nakajima, Y. Honda, O. Kitao, H. Nakai, M. Klene, X. Li, J.E. Knox, H.P. Hratchian, J.B. Cross, V. Bakken, C. Adamo, J. Jaramillo, R. Gomperts, R.E. Stratmann, O. Yazyev, A.J. Austin, R. Cammi, C. Pomelli, J.W. Ochterstki, P.Y. Ayala, K. Morokuma, G.A. Voth, P. Salvador, J.J. Dannenberg, V.G. Zakrzewski, S. Dapprich, A.D. Daniels, M.C. Strain, O. Farkas, D.K. Malick, A.D. Rabuck, K. Raghavachari, J.B. Foresman, J.V. Ortiz, Q. Cui, A.G. Baboul, S. Clifford, J. Cioslowski, B.B. Stefanov, G. Lui, A. Liashenko, P. Piskorz, I. Komaromin, R.L. Martin, D.J. Fox, T. Keith, M.A. Al-Laham, C.Y. Peng, A. Nanayakkara, M. Challacombe, P.M.W. Gill, B. Johnson, W. Chen, M.W. Wong, C. Gonzalez, J.A. Pople, Gaussian03, Revision B.05, Gaussan, Inc., Wallingford, CT, 2004.

[24] T.A. Halgren, J. Comput. Chem. 17 (1996) 490.

[25] T.A. Halgren, J. Comput. Chem. 17 (1996) 520.

[26] N.L. Allinger, Y.H. Yuh, J.H. Lii, J. Am. Chem. Soc. 111 (1989) 8551.

[27] N.L. Allinger, K.S. Chen, J.H. Lii, J. Comput. Chem. 17 (1996) 642.

[28] M.J. Saunders, J. Am. Chem. Soc. 109 (1987) 3150.

[29] T. Kuppens, W. Langenaeker, J.P. Tollenaere, P. Bultinck, J. Phys. Chem. A 107 (2003) 542.

[30] D.A. McQuarrie, Statistical Thermodynamics, Harper and Row, New York, 1973.

[31] R.D. Johnson III (Ed.), NIST Standard Reference Database No. 101, Release May 11, 2005, http://srdata.nist.gov//cccbdb.

[32] K.J. Miller, J.A. Savchik, J. Am. Chem. Soc. 101 (24) (1979) 7206.

[33] P. Španěl, M. Pavlik, D. Smith, Int. J. Mass Spectrom. Ion Process. 147 (1995) 177.

[34] D. Smith, A.D. Diskin, Y.F. Ji, P. Španěl, Int. J. Mass Spectrom. 209 (2001) 81.

[35] H.-D. Martin, C. Heller, B. Mayer, H.-D. Beckhaus, in Gas phase Ion Energetics Data, compiled by S.G. Lias, J.F. Liebman, in: P.J. Limstrom, W.G. Mallard (Eds.), NIST Chemistry WebBook, NIST Standard Reference Database 69, National Institute of Standards and Technology, Gaithersburg, MD, 2005, http://webbook.nist.gov.

[36] D. Smith, T. Wang, P. Španěl, Int. J. Mass Spectrom. 230 (2003) 1.

[37] G. De Petris, A. Di Marzio, F. Grandinetti, J. Phys. Chem. 95 (1991) 9782.

[38] U.S. Secretary of Commerce on behalf of the U.S.A., Mass spectrum, in: P.J. Limstrom, W.G. Mallard (Eds.), NIST Chemistry WebBook, NIST Standard Reference Database 69, National Institute of Standards and Technology, Gaithersburg, MD, 2005, http://webbook.nist.gov.

[39] T. Wang, P. Španěl, D. Smith, Int. J. Mass. Spectrom. 228 (2003) 117.

[40] A. Tani, S. Hayward, C.N. Hewitt, Int. J. Mass Spectrom. 223/224 (2003) 561.